Adsorption of humic acid fractions by a magnetic ion exchange resin

Ding, Lei; Wanga, Dandan ; Li, Ling ; Jia, Yunhan ; Ma, Jiangya ; Wang, Feifei; van der Hoek, Jan Peter

DOI
10.2166/wst.2022.076

Publication date
2022

Document Version
Final published version

Published in
Water Science and Technology

Water Science & Technology

Water Science & Technology Vol 85 No 7, 2129 doi: 10.2166/wst.2022.076

Adsorption of humic acid fractions by a magnetic ion exchange resin

Lei Ding[a,b,†], Dandan Wang[a,b,†], Ling Li[b], Yunhan Jia[b], Jiangya Ma[b], Feifei Wang[a,c,*] and Jan Peter van der Hoek[d,e]

[a] Engineering Research Center of Biomembrane Water Purification and Utilization Technology, Ministry of Education, Anhui University of Technology, Maanshan 243002, China
[b] School of Civil Engineering and Architecture, Anhui University of Technology, Maanshan 243002, China
[c] School of Environmental and Chemical Engineering, Shanghai University, Shanghai 200444, China
[d] Department of Water Management, Delft University of Technology, 2628 CN Delft, The Netherlands
[e] Waternet, Research & Innovation Program, 1096 AC Amsterdam, The Netherlands
*Corresponding author. E-mail: wff1986@163.com
[†]These two authors contributed equally to this work.

ABSTRACT

Natural organic matter in waters varies in different fractions. To better understand the removal of different fractions by a magnetic ion exchange (MIEX) resin and the mechanism behind it, this study investigated adsorption kinetics, equilibrium and thermodynamics of humic acid (HA) fractions with different hydrophilic–hydrophobic properties and molecular weights on MIEX resin through a series of batch experiments. MIEX resin can effectively remove approximately 40% of hydrophilic and 30% of hydrophobic HA components, as well as approximately 44% of molecular weight (MW) <10 kDa to some degree. The removal efficiency of HA fractions by MIEX resin reduced with the increase of pH from 6 to 9. Adsorption kinetics of different HA fractions on MIEX resin fitted the pseudo-second-order model well. With the increase of MW of HA from <1 kDa to >10 kDa, the time to reach adsorption equilibrium reduced from 180 to 120 min. It took more time for the hydrophilic fractions (140 min) to reach the equilibrium than for hydrophobic HA fractions (120 min). The Sips model fitted the adsorption equilibrium data of HA fractions on MIEX resin well. It was revealed that the adsorption of HA fractions on MIEX resin was spontaneous, endothermic and an entropy driven process, and the chemisorption might dominate the adsorption of HA components on MIEX resin. This study is of great significance to the design of magnetic ion exchange resin reactors and the optimization of operational parameters for the removal of natural organic matter with different hydrophilic–hydrophobic properties and molecular weights in different water sources.

Key words: adsorption, HA, ion exchange, MIEX resin, molecular weight

HIGHLIGHTS

- MIEX resin can remove hydrophilic and hydrophobic HA and MW <10KDa HA.
- The removal of 8 HA fractions by MIEX resin decreases with pH increase.
- The equilibrium time is related to hydrophobicity and MW of HA.
- The equilibrium time decreases with the increase in MW of HA fractions.
- Kinetics and adsorption equilibrium models were established.

GRAPHICAL ABSTRACT

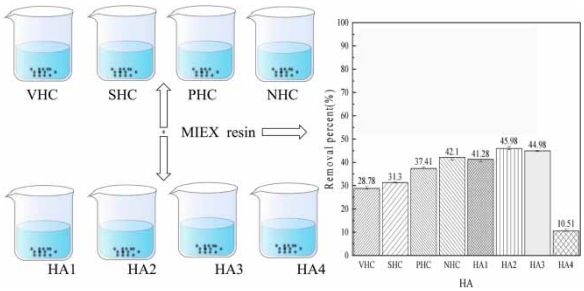

1. INTRODUCTION

Natural organic matter (NOM) exists extensively in natural surface water sources because of the breakdown of animal and/or plant biomass residues (Phetrak *et al.* 2016; Asgharian *et al.* 2017; Geoffrey 2018). HA is the representative substance of NOM, accounting for 50–90% of the total natural organic compounds in water sources (Wang *et al.* 2017). HA is the main cause of water color and odor. Furthermore, HA can interact with toxic organic compounds and heavy metal ions and therefore influence the distribution and migration of organic matter and metal ions by hydrophobic distribution, adsorption, charge transfer and static repulsion (Ren *et al.* 2017; Rajaei *et al.* 2021). More seriously, during drinking water disinfection, HA can react with chlorine to produce various by-products which are potentially carcinogenic, deformed and mutated (Bond *et al.* 2010). Hence, eliminating HA from water sources prior to chlorination is essential for water safety and human health.

Usually, coagulation/sedimentation/filtration (Zhang *et al.* 2017), biological activated carbon filtration (Liu *et al.* 2020) and ion exchange (Cornelissen *et al.* 2009) are the three most used technologies to removal HA from waters. MIEX resin is a strong base resin with chloride as the exchangeable ion, equipped with macro-porous polyacrylic matrix and marketed by Orica Watercare (Ding *et al.* 2012a; Yang *et al.* 2020). The adsorption of HA on MIEX resin is one of the most excellent and economical methods applied in recent years owing to its two merits (Singer & Bilyk 2002; Mergen *et al.* 2008; Ding *et al.* 2012a; Gibert *et al.* 2017): 1) small particle size (150–180 μm, 2–5 times smaller than traditional resin) allowing HA to be removed quickly; 2) magnetic performance (γ-Fe_2O_3 being incorporated into its matrix) enhancing the separation of saturated MIEX resin from water.

Previous research has proven that MIEX resin can remove around 50% NOM (Drikas *et al.* 2011; Nguyen *et al.* 2011; Phetrak *et al.* 2014). It was also observed that MIEX removed 20–34% dissolved organic carbon (DOC) and 30–48% UV from landfill leachate (Singh *et al.* 2012). Boyer & Singer (2005) reported maximum removal of 36–72% DOC and 54–83% UV by MIEX resin. Under suitable conditions, the removal of HA could reach 70–80% (Ren & Graham 2015; Lu *et al.* 2016). The reported differences in the removal efficiency of NOM in different raw waters may be attributed to the difference in NOM fractions in water matrices as well as the experimental conditions. Actually, some studies also showed that the adsorption efficiency of NOM on MIEX resin was related to the properties of NOM fractions (hydrophilicity and MW). Singer & Bilyk (2002) found that MIEX resin appeared to be effective for the removal of both hydrophilic and hydrophobic fractions of NOM. Mergen *et al.* (2008) and Nguyen *et al.* (2011) reported that most of the hydrophilic components could be preferentially removed by MIEX resin, while Drikas *et al.* (2011) and Watson & Knight (2014) found that MIEX adsorbed a larger portion of hydrophobic components than hydrophilic components. Regarding the removal of HA fractions with different molecular weights, a previous study (Allpike *et al.* 2005) showed that MIEX resin was the best material to remove the MW 1–5 kDa fraction. Another study (Phetrak *et al.* 2014) also demonstrated that MIEX resin could remove the MW 1–4 kDa fraction rather than the MW <1 kDa fraction of NOM. However, Humbert *et al.* (2005) found that the intermediate MW (500–1,500 Da) fraction was well removed by MIEX resin. Although, the reported results above proved that the hydrophilic–hydrophobic properties and the MW of NOM compounds in raw water affected the removal efficiency of NOM by MIEX resin, it is controversial about what property HA components can be removed effectively. Furthermore, the removal results of different NOM fractions by MIEX resin were mainly described qualitatively in most of the previous literature. In contrast, few quantitative results on the removal of NOM fractions by MIEX resin have been reported up to now, limiting the application of the MIEX resin reactor in different water sources all over the world due to different dominant NOM fractions. Therefore, the quantitative results, such as the adsorption kinetics, equilibrium, thermodynamic characteristics of different NOM fractions with different hydrophilicity and/or MW, should be given and are crucial for the design of MIEX resin reactors.

Accordingly, the aim of this study was to provide the fundamental data and guide for the design of the MIEX reactor used to remove NOM with different hydrophilic–hydrophobic properties and molecular weights in different water sources. The specific objectives were to: (1) investigate the removal efficiency of HA fractions in terms of different hydrophilic–hydrophobic properties and molecular weight by MIEX resin for different environmental factors; (2) establish the kinetics and equilibrium model equations of the different HA fractions adsorbed on MIEX resin; (3) explore the thermodynamics characteristics of the adsorption process by energy change.

2. MATERIALS AND METHODS

2.1. Materials

Supelite DAX-8 resin, Amberlite XAD-4 resin, Amberlite IRA-958 resin and commercial HA were purchased from Sigma (America). Solid phase extraction (SPE) equipment (QYCJ-12D, Shanghai Qiaoyue Electronics Co., Ltd, China) and the columns (C18, Shanghai Qiaoyue Electronics Co., Ltd, China) were used to separate HA into hydrophobic and hydrophilic fractions. A Polyether Sulfone Ultrafiltration membrane (PES) and an ultrafiltration device (MSC300, Shanghai Mosu Science Equipment Co., Ltd, China) were used to separate HA into different MW fractions. MIEX resin was supplied by China Agent of Orica Watercare. The resin particles' properties are given in Table 1 (Phetrak *et al.* 2014). Solution pH was adjusted using either 0.1 M HCl or 0.1 M NaOH. Alcohol (75%) was bought from Guangzhou Jinwang Chemical Co. Ltd, China. All chemicals were guaranteed reagent grade.

2.2. Preparation of dissolved HA

1 g HA was added into a beaker containing 500 mL ultrapure water, and the mixture was stirred for 8 h to accelerate the dissolution of HA on a digital display constant temperature magnetic stirrer (H01-1C, Shanghai Mei Yingpu instrument and Meter Manufacturing Co., Ltd, China), followed by filtering through 0.45 μm micro-filtration membranes (Shanghai Xinya Purification Equipment Co., Ltd, China). The filtrate named as the soluble HA was kept in the refrigerator at 277 K before use in subsequent experiments.

2.3. Separation and characterization of HA fractions

2.3.1. HA fractions with different hydrophilicity

According to the hydrophilic and hydrophobic characteristics, HA was separated into four fractions, very hydrophobic compounds (VHC), slightly hydrophobic compounds (SHC), polar hydrophilic compounds (PHC) and neutral hydrophilic compounds (NHC) using SPE with different types of resin (Fan *et al.* 2014; Phetrak *et al.* 2016). The specific separation process was as follows:

Firstly, 500 mL HA solution was acidified to pH = 2 with 0.1 M HCl. The Supelite DAX-8 resin, Amberlite XAD-4 resin and Amberlite IRA-958 resin were soaked in alcohol for 24 hours before being packed in the extraction columns. Secondly, the acidified HA solution flowed through the cleaned column arrays of Supelite DAX-8 resin and Amberlite XAD – 4 resin successively. The effluent solution was adjusted to pH = 8 with 0.1 M NaOH and then flowed through the Amberlite IRA-958 column. The HA fraction in the final effluent was called as NHC. Ultimately, VHC, SHC or PHC in eluent was obtained by rinsing DAX-8 resin, XAD-4 resin and IRA-958 resin with 500 mL 0.1 M NaOH, respectively. After separation, each HA component was adjusted to neutral pH and was saved in the refrigerator at 277 K.

2.3.2. HA fractions with different MW

Ultrafiltration membranes with different pore diameters were equipped to separate the HA solution into different MW fractions (Hua & Reckhow 2007; Shuang *et al.* 2014). The specific separation process was as follows:

The ultrafiltration membranes were firstly soaked in alcohol for 24 h and placed in ultrapure water for standby. The HA solution was sequentially fractionated through PES membrane of 10, 5 and 1 kDa. The HA fraction in the final effluent was called HA1 (MW < 1 kDa). Each membrane above was rinsed with 200 mL 0.1 mol/L NaOH, respectively. The HA fraction in the eluent was classified as: HA4 (MW > 10 kDa), HA3 (MW = 5–10 kDa), HA2 (MW = 1–5 kDa), respectively. Finally, each component was adjusted to neutral pH, and was kept in the refrigerator at 277 K.

2.3.3. Characterization of HA

The DOC concentration was measured with a total organic carbon analyzer (TOC-L, Shanghai Shimadzu Co., Ltd, China). A zeta potential analyzer (MalvernZetasizer Nano ZS90, Malvern Instruments Ltd, England) was used to measure the charge

Table 1 | The characteristics of MIEX resin

Material	Surface area (m^2/g)	Particle pore size (nm)	Particle size (μm)	Capacity (meq/mL)	Water content (%)
Polyacrylic	43.5	2	150–180	0.52 ± 0.02	65 ± 1

potential of HAs. Ultraviolet absorbance was determined at 254 nm (UV_{254}) using an ultraviolet–visible spectrophotometer (UV-9600, Beijing Ruili Analytical Instrument Co., Ltd, China). The specific ultraviolet absorbance ($SUVA_{254}$) value was calculated using Equation (1):

$$SUVA_{254}(L/(mg \cdot m)) = \frac{UV_{254}}{TOC} \tag{1}$$

2.4. Adsorption experiments

2.4.1. Removal efficiency of HA fractions on MIEX resin

Adsorption experiments were undertaken at neutral pH. 2 mL MIEX resin was added into 500 mL beakers containing 200 mL solution with different HA fractions. The experiments were performed in triplicate. The DOC concentration in each HA fraction solution was adjusted to approximately 10 mg/L by diluting prepared HA fraction solutions using ultrapure water (Afshin *et al.* 2021). Then, the mixture of MIEX resin and each HA fraction was agitated for 180 min with a speed of 150 rpm at a temperature of 298 K using a program-controlled jar test apparatus (ZR4-6, Shenzhen Zhong-run Water Industry Technology and Development Co., Ltd, China). After 180 min adsorption, the mixtures were filtered using 0.45 μm Millipore membranes. The DOC concentration in the filtrate was determined with 5 mL solution.

The removal efficiency (E) of each HA fraction by MIEX resin was calculated by Equation (2):

$$E(\%) = \frac{C_0 - C_t}{C_0} \times 100 \tag{2}$$

where C_0 (mg/L) and C_t (mg/L) represent the concentration of DOC at initial and time t, respectively. E is the removal efficiency of each HA fraction on MIEX resin.

2.4.2. Effect of solution pH

The effect of initial solution pH on the removal of different HA fractions was explored by varying solution pH from 6 to 9 using 0.1 M HCl or NaOH. The adsorption procedure was similar to that described in Section 2.4.1.

2.4.3. Adsorption kinetics

Adsorption kinetics experiments of eight HA fractions were carried out at 298 K and neutral solution pH. Taking a specific HA fraction as an example to describe the experimental process, 2 mL MIEX resin was added into a beaker containing 200 mL solution with the HA fraction of approximately 10 mg/L DOC. Then the mixture was agitated mechanically at 150 rpm on the program-controlled jar test apparatus. The samples were taken from the beaker after 5, 10, 15, 20, 30, 40, 50, 60, 90, 120, 150, 180, 210 and 240 min. Before the DOC was measured, the water samples were filtered using 0.45 μm Millipore membranes firstly. All experiments were performed in triplicate.

At time t, the amount of each HA fraction adsorbed on MIEX resin (q_t, mg/mL) was calculated using formula (3):

$$q_t = \frac{V(C_0 - C_t)}{W} \tag{3}$$

The amount of each HA fraction adsorbed on MIEX resin at equilibrium (q_e, mg/mL) was calculated using formula (4):

$$q_e = \frac{V(C_0 - C_e)}{W} \tag{4}$$

where C_0 (mg/L), C_t (mg/L) and C_e (mg/L) represent DOC in HA fraction solution at initial, time t and equilibrium, respectively; V (L) is the volume of solution and W (mL) is the volume of MIEX resin.

The pseudo-first-order kinetic model and pseudo-second-order kinetic model were applied to simulate the dynamic process. Data analysis was accomplished by Origin 8.0.

The pseudo-first-order kinetic model is widely used, and it assumes that, besides the change of adsorption rate, the adsorption of adsorbates is in proportion to the amount of adsorption and equilibrium adsorption capacity (Largitte & Pasquier 2016). The model is shown as Equation (5):

$$q_t = q_e(1 - \exp(-k_1 t)) \tag{5}$$

The pseudo-second-order kinetic model is closely related to chemical adsorption, and this chemical adsorption involves electron sharing and electron transfer between adsorbent and adsorbate (Shuang *et al.* 2012a). Its expression is shown as Equation (6):

$$q_t = \frac{k_2 q_e t}{1 + k_2 q_e t} \tag{6}$$

where k_1(mg/(mL·min)) is the kinetic constant for the model of the pseudo-first-order; k_2(mg/(mL·min)) is the kinetic constant for the model of the pseudo-second-order.

2.4.4. Adsorption equilibrium

The adsorption equilibrium experiments with eight HA fractions were conducted at 293, 303 and 313 K, respectively. 2 mL MIEX resin was added into 500 mL beakers containing 200 mL solution with different HA fractions. The DOC concentration in each HA fraction solution ranged from 2 mg/L to 15 mg/L. The experimental procedure was similar to that described in Section 2.4.1.

The Langmuir isotherm model, Freundlich isotherm model and Sips isotherm model were applied to simulate the adsorption equilibrium process. Data analysis was accomplished by Origin 8.0.

The Langmuir isotherm model assumes that the adsorption potential of adsorbent on the resin surface is equal to each other and the adsorbate is monolayer distributed (Tang *et al.* 2014). The Langmuir isotherm model is provided in Equation (7) (Ayub *et al.* 2019):

$$q_e = \frac{q_m K_s C_e}{1 + K_s C_e} \tag{7}$$

where q_m (mg/mL) is maximum monolayer adsorption capacity of each HA fraction on MIEX resin; K_s (L/mg) is the constant of Langmuir model and related to the adsorption free energy between adsorbent and adsorbate.

The Freundlich isotherm model is widely used in complex adsorption systems (Llorca *et al.* 2018), and its mathematical expression is shown in Equation (8):

$$q_e = K_e C_e^{1/n} \tag{8}$$

where K_e (mg/mL(L·mg)$^{1/n}$) is the constant of the model, which is related to the binding energy and the adsorption capacity; 1/n is a heterogeneity factor.

Sips isotherm model (Tzabar & Ter Brake 2016) is a typical hybrid model, which can be used to predict heterogeneous systems, and its mathematical expression is shown in Equation (9):

$$q_e = \frac{K_c C_e^{B_m}}{1 + A_m C_s^{B_m}} \tag{9}$$

where K_c (L/mL) and A_m (L/mg) are constants of the model; B_m is the exponent of the model.

2.4.5. Thermodynamics

According to the laws of thermodynamics, ΔH^0 and ΔS^0 is independent of temperatures, the relationship between the ΔG^0 parameter and the others (ΔH^0 and ΔS^0) is expressed as follows (Altunterim & Vergili 2020):

$$\ln K_{eq} = \frac{\Delta S^0}{R} - \frac{\Delta H^0}{RT} \tag{10}$$

$$\Delta G^0 = \Delta H^0 - T\Delta S^0 \tag{11}$$

where K_{eq} is the thermodynamic equilibrium constant, the value of K_c is used here (Tran *et al.* 2021); R (8.314 J/(mol·k)) is the gas constant; T is the absolute temperature.

2.4.6. Activation energy

The adsorption kinetics of eight HA fractions on MIEX resin were determined at 293, 303 and 313 K, respectively. The experimental procedure of each HA fraction is similar to that described in Section 2.4.3. The activation energy (E_a, kJ/mol) of each HA fraction adsorbed on MIEX resin can be calculated according to Equation (12) (Ding *et al.* 2017):

$$lnk_2 = \ln A - \frac{E_a}{RT} \tag{12}$$

where k_2 (mg/(mL·min)) is the reaction rate constant; A (mol/(L·s)) is a pre index factor.

3. RESULTS AND DISCUSSION

3.1. Removal of different HA fractions by MIEX resin

Figure 1 illustrates the removal effectiveness of different HA fractions by MIEX resin. For the HA components with different MW, removal percentages of HA1 (MW < 1 kDa), HA2 (MW = 1–5 kDa) and HA3 (MW = 5–10 kDa) were 41.28%, 45.98%, and 44.98% respectively, which had no apparent difference. The removal efficiency of HA4 (MW > 10 kDa), however, dropped dramatically to an unexpected level of 10.61%. This indicates that MIEX resin preferentially removes the low MW fraction (MW < 10 kDa) instead of the high MW (>10 kDa) fraction. This finding agrees with previous literature reporting that MIEX resin removed much low-mid MW fractions: around 80% 1–10 kDa fraction and 60% <1 kDa fraction (Banks *et al.* 2004; Boyer & Singer 2005). The reason why the removal percentage of MW > 10 kDa HA component by MIEX resin was much less than that of low MW fractions may be attributed to the fact that large MW HA fractions can be removed mainly by external active sites instead of inner active sites of resin particles. The large MW HA molecules with large sizes, adsorbing on active sites of resin particles, covered much of the external surface of the resin particles. This causes

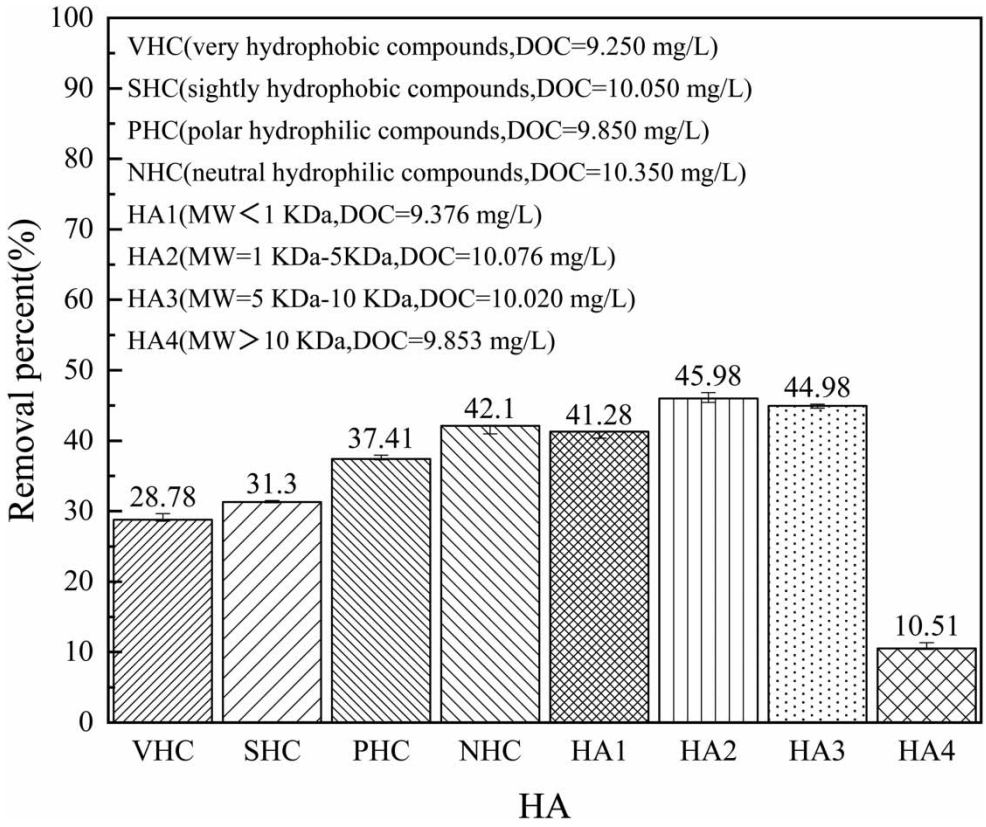

Figure 1 | Removal percentages of different HA fractions on MIEX resin.

the entrance to the inner pores of the resin to be blocked and, therefore, the inner pores are not available for adsorption. (Boyer & Singer 2005; Shuang *et al.* 2012b; Singh *et al.* 2012).

For the hydrophobic or hydrophilic HA components, Figure 1 shows that the removal percentages of VHC (28.76%) and SHC (31.30%) by MIEX resin were extremely close, while removal percentages of PHC (37.41%) and NHC (42.1%) were higher than those of VHC and SHC. These results show that MIEX resin can remove both hydrophobic and hydrophilic HA components. The removal of hydrophilic components is more effective than that of hydrophobic components by MIEX resin, implying that MIEX resin exhibits more preferential affinity for hydrophilic components. Singer & Bilyk (2002) found that MIEX resin appeared to be effective for the removal of both hydrophobic and hydrophilic carbon, but specially pointed out that it did not mean that MIEX resin had no preferential difference for the removal of hydrophilic and hydrophobic components. Zhang *et al.* (2006) reported that MIEX resin could remove a majority of hydrophilic compounds and a significant amount of hydrophobic compounds from biologically treated secondary effluent, with the TOC removal efficiency of 69.1% and 56.5% respectively, which means that MIEX resin has preferential affinity for hydrophilic compounds. The difference in zeta potential of four hydrophilic and hydrophobic HA fractions may cause MIEX resin to be more effective for removing hydrophilic HA fractions than hydrophobic HA fractions. Zeta potentials of four HA fractions in this study are given in Table 2. As shown in Table 2, the zeta potentials of VHC, SHC, PHC, and NHC are −22.2, −24.8, −25.6 and −26.0 mV, respectively. All zeta potential values are negative, meaning that these HA fractions can be adsorbed onto MIEX resin (as anion exchange resin) by exchanging with chloride ion. In contrast, the zeta potentials of hydrophilic HA fractions (PHC and NHC) are more negative than those of hydrophobic components (VHC and SHC), causing more preferential affinity and higher removal efficiency. In addition, the difference in the MW of the hydrophobic and hydrophilic compounds might be another reason for the different removal efficiencies. The hydrophobic organic compounds were more likely to consist of larger MW components (Boyer *et al.* 2008; Nguyen *et al.* 2011). This resulted in size exclusion and channel blocking of MIEX resin and, therefore, decreased the removal of hydrophobic HA fractions by resin.

Accordingly, compared with previous literatures, this study demonstrated definitely that MIEX resin could remove effectively HA components of MW < 10 kDa; also, in contrast, MIEX resin exhibited more preferential affinity for hydrophilic components than hydrophobic components. However, for hydrophilic components, the reasons (differences in MW of organic matter or negative charges) causing better removal on MIEX resin are unclear and need to be investigated in future study.

3.2. Effect of solution pH

The effect of solution pH on the removal of HA fractions with different MW and hydrophobicity by MIEX resin was investigated, and the results are given in Figure 2. Figure 2 showed that for all HA fractions, the removal efficiency decreased with the increase in solution pH from 6 to 9. The hydroxyl ions which usually increase with the increase of solution pH compete for adsorption sites with HA fractions. This might cause the decrease in removal efficiency under the high pH conditions. In addition, the ionization degree of HA fractions is more complete at alkaline environment, and the electrostatic repulsion between the HA molecules in solution and on the surface of MIEX resin impedes the diffusion of HA molecules onto the surface of MIEX resin (Xu *et al.* 2016). This might be another reason causing a declined removal efficiency at alkaline conditions. In addition, the shape of HA molecules might expand in alkaline conditions (Avena & Koopal 1999) and therefore these HA molecules, adsorbed on the surface of MIEX resin, cover more adsorption sites. The decrease in available adsorption sites results in the reduction of HA removal efficiency by MIEX resin.

Figure 2 also displays that for the MW < 1 kDa HA fraction, the removal efficiency by MIEX resin decreased only slightly with the increase of pH in contrast to the other fractions, implying the inappreciable effect of solution pH change on the

Table 2 | Zeta potential of HA fractions

HA	Zeta potential (mV)	SUVA value (L/(mg·m))
VHC	−22.2	10.03
SHC	−24.8	4.03
PHC	−25.6	0.13
NHC	−26.0	0.09

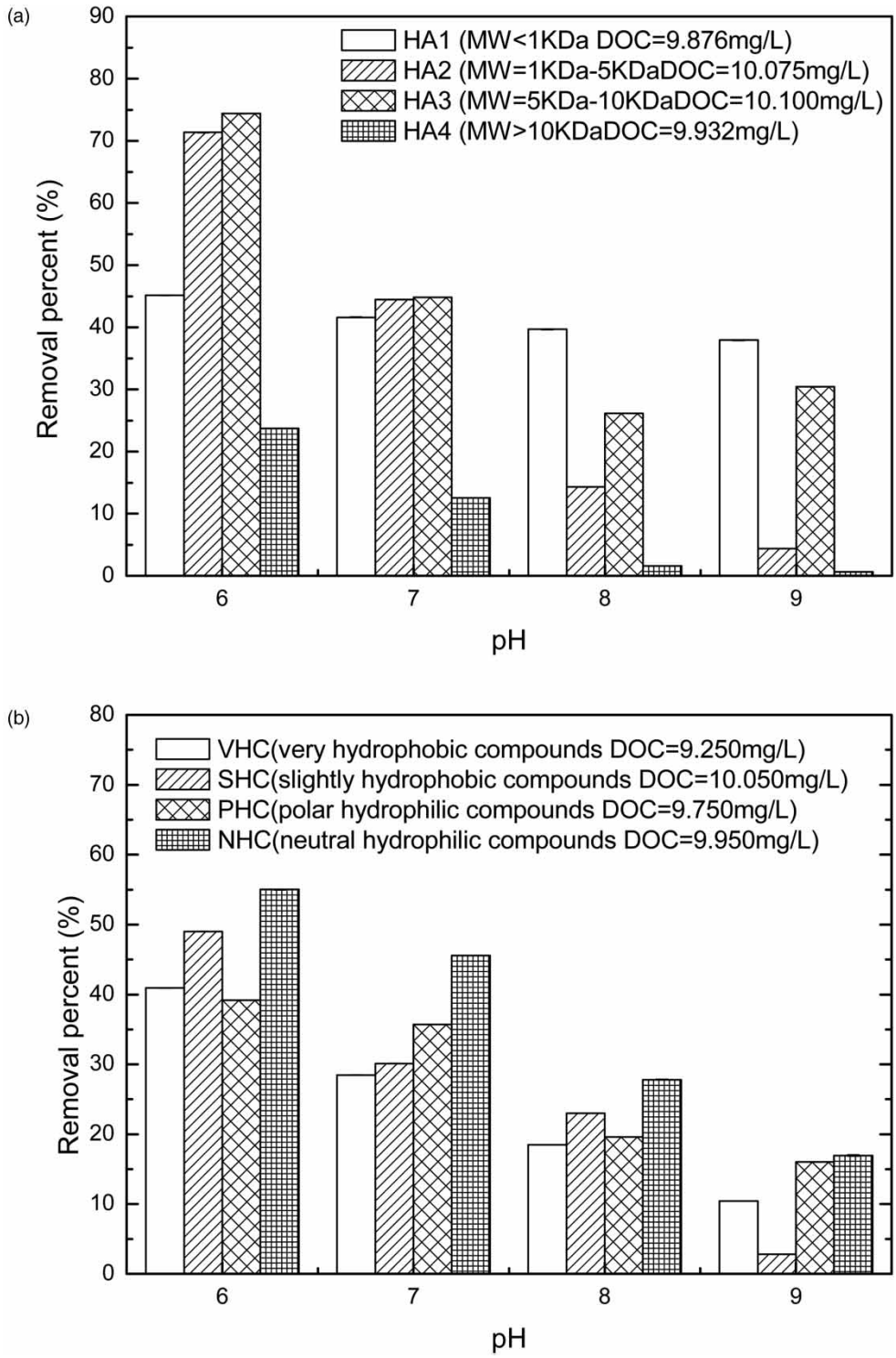

Figure 2 | Effect of pH on removal of HA with different properties by MIEX resin.

removal of MW < 1 kDa fraction. Accordingly, it is unnecessary to adjust solution pH when MIEX resin is used to remove the small molecular HA components (MW <1 kDa). However, when MIEX resin is used to remove other HA fractions, solution pH has to be adjusted in order to achieve effective removal.

3.3. Adsorption kinetic study

Adsorption kinetics data of eight HA fractions on MIEX resin are given in Figure 3. The removal rate of each HA fraction increased rapidly in the initial stage of adsorption, then increased slowly with time, and finally reached equilibrium with approximately equivalent removal efficiencies. At the initial stage, a large number of available adsorption sites on the surface of MIEX resin led to a sharp increase of HA removal. Afterwards, available active sites on the surface of MIEX resin gradually decreased with time. The diffusion speed of HA onto MIEX resin also decreased with time due to the decline in HA concentration gradient between bulk solution and resin surface. The two reasons led to a reduction in HA removal rate with time (Ding *et al.* 2012b). With the available sites being exhausted, the equilibrium was achieved.

Figure 3(a) showed that it took about 120 min for the HA fractions with MW = 1–5 kDa and MW = 5–10 kDa to achieve equilibrium. The time for the MW > 10 kDa fraction to reach equilibrium on MIEX resin was about 30 min less than that for the other fractions. It is worth noting that, for the MW < 1 kDa HA fraction, the removal by MIEX resin reached equilibrium after 180 min adsorption. The results mean that the adsorption equilibrium time of HA fractions by MIEX resin is related to MW of HA fractions. The HA fractions with large MW (>10 kDa) are difficult to diffuse into the internal pores of MIEX resin, and mainly adsorbed on the external adsorption sites within short time. In contrast, the adsorption rate on external surface is much quicker than the diffusion rate in the internal pore path (Shuang *et al.* 2015). This might be the reason why it needed less time to attain adsorption equilibrium for MW > 10 kDa HA fractions. For medium MW HA fractions (MW = 1–10 kDa), some molecules can diffuse into pores to be adsorbed on internal sites besides surface adsorption, extending the equilibrium time. Small MW HA fractions (<1 kDa) need much longer diffusion time, leading to the adsorption equilibrium achieved after 180 min.

Also, Figure 3(b) reveals that it took about 140 min for fractions PHC and NHC, and a little shorter for VHC and SHC (120 min). The difference in time to reach equilibrium for the hydrophobic fractions compared to the hydrophilic fractions might be due to the disparity in MW. The very hydrophobic HA fractions are composed of large MW organics, mainly being adsorbed on external surfaces (Schlenger *et al.* 2016). Nevertheless, the hydrophilic HA fractions consist of small MW organics, diffusing into internal pore channels (Schlenger *et al.* 2016).

Previous studies using MIEX resin for organics removal from raw water showed that most dissolved organic matter and UV_{254} can be removed within 15–30 min (Singer & Bilyk 2002; Banks *et al.* 2004; Boyer & Singer 2005; Phetrak *et al.* 2014; Xu *et al.* 2016). Nguyen *et al.* (2011) found that for the organics in the effluent of a biological wastewater treatment, the majority of DOC was removal by MIEX resin in the first 30–60 min. This study did a further investigation regarding the equilibrium of the different HA fractions. The finding that the equilibrium time depends on the organics' characteristics, i.e. MW and/or hydrophobicity, implies that the optimal contact time of MIEX resin should be selected based on the MW and hydrophilic–hydrophobic properties of dominant organic components in raw water during water and wastewater treatment by MIEX resin.

The adsorption kinetic equations of different HA fractions on MIEX resin are crucial for designing process equipment and elucidating the adsorption mechanism (Ding *et al.* 2012a). The fitting results of the pseudo-first-order model and pseudo-second-order model are revealed in Table 3. Table 3 demonstrates that the pseudo-second-order model simulated the adsorption kinetic process of all HA fractions better than the pseudo-first-order model. The calculated q_e values (cal) are almost the same with the experimental q_e values (exp), suggesting that the adsorption kinetic process follows the pseudo-second-order kinetic model.

3.4. Adsorption isotherms study

The adsorption equilibrium experiments of eight HA components on MIEX resin were conducted at 293 K, 303 K, 313 K, and the results are given in Figure 4.

Figure 4 displays that the higher the concentration and the temperature, the larger the absorption capacity. It may be explained by the fact that the concentration gradient between the solution and the resin accelerates the HA molecules to enter the internal pores of the resin and occupy more adsorption positions, and the higher temperature is beneficial to decreasing the viscosity of HA solution and increasing the HA diffusion rate into MIEX resin pores. The increase in adsorption capacity with elevating temperature implies that the adsorption processes of HA components on MIEX resin are endothermic reactions. Figure 4 shows that the influence of the temperature on the removal of different MW components is more intense than that of hydrophilic–hydrophobic properties.

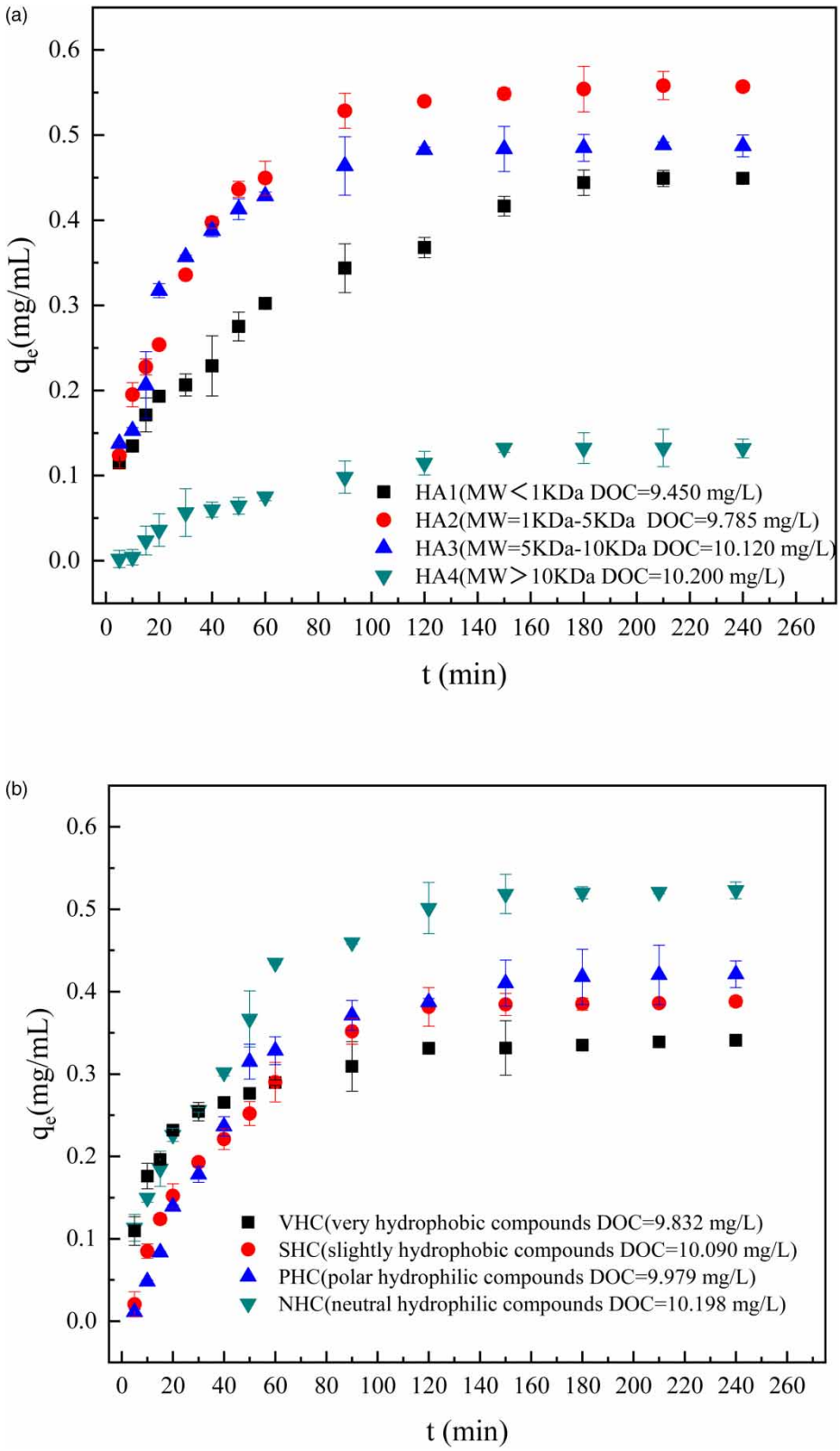

Figure 3 | Adsorption kinetics of different HA fractions onto MIEX resin.

Table 3 | Kinetics parameters of different HA fractions onto MIEX

	Pseudo-first-order model					Pseudo-second-order model				
HA	k_1 (mg/(mL·min))	q_e(cal) (mg/mL)	q_e(exp) (mg/mL)	R^2	SE (%)	k_2 (mg/(mL· min))	q_e(cal) (mg/mL)	q_e(exp) (mg/mL)	R^2	SE (%)
VHC	0.059	0.34	0.34	0.87	0.76	0.3538	0.25	0.34	0.98	0.4
SHC	0.0225	0.39	0.39	0.99	0.5	0.0493	0.48	0.39	0.98	1.43
PHC	0.0206	0.43	0.42	0.98	1.15	0.0365	0.54	0.42	0.96	3.11
NHC	0.0260	0.52	0.52	0.98	0.97	0.0453	0.62	0.52	0.98	1.84
HA1	0.0219	0.43	0.45	0.93	1.6	0.0467	0.52	0.45	0.96	2.01
HA2	0.0323	0.55	0.56	0.99	0.7	0.0619	0.64	0.56	0.98	1.2
HA3	0.0423	0.48	0.49	0.98	0.68	0.1006	0.54	0.49	0.96	1.46
HA4	0.0133	0.14	0.13	0.98	0.54	0.0574	0.19	0.13	0.97	1.28

As showed in Table 4, the Langmuir model, Freundlich model and Sips model were applied to fit the adsorption equilibrium data of HA components on MIEX resin. Among the three models, the adsorption equilibrium of each component on MIEX resin can be described best by the Sips model at any temperature, with the greatest R^2 (more than 0.97) and the least standard error. Moreover, the poor fitting results of the Langmuir model also showed that ion exchange may not be exclusive. In Shuang's (Shuang *et al.* 2012b) research, the adsorption mechanism of HA on MIEX resin includes electrostatic attraction, electrostatic exclusion, cation–π bonding, π–π interaction in addition to ion exchange. Ion exchange and physical adsorption have also been reported by Phetrak (Phetrak *et al.* 2016). The Sips isotherm model with three parameters is a hybrid of the Langmuir and Freundlich models. This may be the reason why the adsorption equilibrium of HA fractions on MIEX resin fitted the Sips isotherm model well.

3.5. Thermodynamics study

The adsorption reaction of HA fractions on MIEX resin is accompanied by the absorption and release of heat. The study of adsorption thermodynamics is helpful to further understand the thermodynamic characteristics of adsorption behavior and to reveal the adsorption mechanism. K_{eq} is the thermodynamic equilibrium constant, the linear fitting was performed with $\ln K_{eq}$ against 1/T. The slope was the value of ΔH^0, and the intercept was the value of ΔS^0. ΔG^0 as calculated by Equation (11), and as tabulated in Table 5.

As showed in Table 5, all values of ΔH^0 were observed to be positive, indicating that the adsorption reaction of all components on MIEX resin was an endothermic process. This can well explain why the increase of temperature was conducive to the adsorption of HA fractions onto MIEX resin (Section 3.4). ΔS^0 values are all positive, implying an increase in the degree of confusion on the solid–liquid interface after adsorption. This suggests that the adsorption of different HA fractions on MIEX resin occurred spontaneously (Tan *et al.* 2009), as is known that the larger the value of ΔS^0, the easier the adsorption occurs (Ding *et al.* 2017). Obviously, ΔS^0 value of HA3 was larger than those of HA1 and HA2, indicating that the spontaneous reaction of the high MW HA fraction on MIEX resin was easier. Simultaneously, the negative values of ΔG^0 imply that these adsorption processes of different HA fractions on MIEX resin were all spontaneous at all temperatures (Torab-Mostaedi *et al.* 2013). For each HA component, ΔG^0 reduced gradually with the increase in the temperature from 293 to 313 K. This shows that the spontaneous reaction was enhanced by increasing temperature. The larger the MW of HA, the more negative the ΔG^0 value. The more negative ΔG^0 means that the adsorption occurs more easily. This indicates that high MW organics will be preferentially adsorbed on the surface of resin and therefore block the pores. As a result, the active adsorption sites of internal pores cannot be fully utilized. Therefore, it may be necessary to remove macromolecular organic matter before MIEX resin treatment in order to make full use of internal adsorption sites of MIEX resin.

3.6. Activation energy

Activation energy (E_a, kJ/mol) can be used to determine the type of adsorption (Bhaumik *et al.* 2015). In order to calculate the activation energy of MIEX resin for the removal of different HA fractions, the removal kinetics of HA fractions by MIEX resin at different temperatures (293 K, 303 K, 313 K) were studied. Based on Equation (13), the E_a values are the slopes and given in Table 6. El-Shahawi & Nassif (2003) reported that when E_a was in the range of 8.4–83.7 kJ/mol, the adsorption was

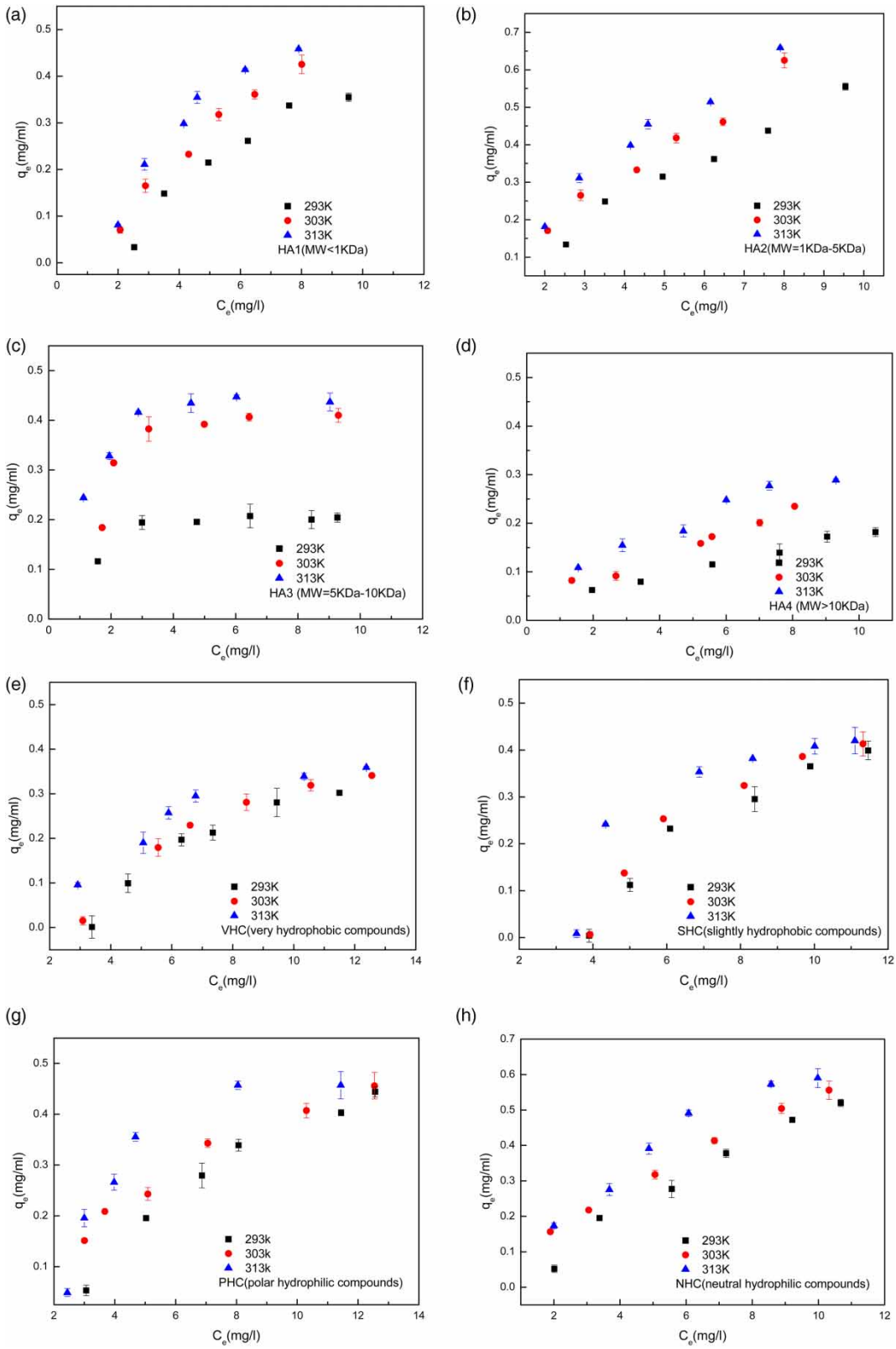

Figure 4 | Adsorption isotherms of different HA fractions onto MIEX.

Table 4 | Isotherm parameters of different HA fractions onto MIEX

		Langmuir model				Freundlich model				Sips model				
HA	Temperature	q_m (mg/mL)	K_s (L/mg)	R^2	SE	$K_e/10^{-2}$ (mg/mL(L·mg)$^{1/n}$)	n	R^2	SE (%)	$K_c/10^{-2}$ (L/mL)	$A_m/10^{-2}$ (L/mg)	B_m	R^2	SE (%)
VHC	293 K	3.83	0.0074	0.92	12.41	2.77	1.02	0.91	1.35	0.03	0.08	4.03	0.98	0.01
	303 K	0.83	0.0573	0.86	0.30	6.34	1.48	0.83	1.53	0.02	0.05	4.43	0.99	0.02
	313 K	1.10	0.0403	0.97	0.44	4.78	1.24	0.96	1.35	0.87	2.23	2.50	0.99	0.23
SHC	293 K	5.77	0.0068	0.96	9.38	4.11	1.05	0.96	0.72	0.12×10^{-3}	0.32×10^{-3}	7.28	0.99	3.47×10^{-4}
	303 K	11.89	8.7889	0.79	94.63	4.13	1.00	0.79	1.62	0.12×10^{-2}	0.31×10^{-2}	6.20	0.97	2.15×10^{-3}
	313 K	1.65	0.0360	0.86	1.72	6.56	1.20	0.86	2.82	0.60×10^{-2}	0.16×10^{-5}	12.60	0.99	0.40×10^{-5}
PHC	293 K	3.92	0.0101	0.83	5.42	4.09	1.06	0.95	1.01	0.27	0.59	2.98	0.99	0.24
	303 K	2.85	0.0192	0.83	4.65	5.40	1.06	0.82	0.97	1.15	2.79	2.75	0.98	0.37
	313 K	2.97	0.0222	0.75	7.28	6.13	1.04	0.75	3.51	2.11	0.23	4.70	0.98	0.10
NHC	293 K	3.56	0.0164	0.98	2.82	6.03	1.08	0.97	0.98	3.12	4.42	1.72	0.99	1.92
	303 K	0.92	0.1062	0.97	0.18	9.77	1.37	0.99	0.15	9.29	−9.26	0.59	0.99	0.17
	313 K	1.63	0.0645	0.98	0.42	11.21	1.30	0.97	1.85	7.45	8.89	1.49	0.99	1.95
HA1	293 K	1.84	0.0267	0.98	0.75	5.27	1.14	0.98	0.51	0.70	2.20	2.63	0.98	1.20
	303 K	1.87	0.0456	0.79	1.00	4.21	0.86	0.96	0.79	1.94	3.04	2.02	0.98	0.72
	313 K	1.96	0.0414	0.90	1.57	8.32	1.16	0.88	2.08	1.47	2.84	2.72	0.99	0.19
HA2	293 K	0.90	0.1088	0.98	0.10	0.12	1.60	0.97	0.87	7.16	11.51	1.36	0.97	8.32
	303 K	3.84	0.0221	0.98	2.56	0.90	1.11	0.98	0.82	9.30	3.99	0.78	0.98	1.04
	313 K	2.50	0.0440	0.98	0.65	0.12	1.21	0.98	1.13	8.84	7.24	1.33	0.98	2.09
HA3	293 K	0.28	0.4610	0.97	0.02	10.31	2.46	0.91	1.10	4.80	24.50	3.87	0.99	0.03
	303 K	0.55	0.4943	0.80	0.08	20.84	2.54	0.77	3.40	0.53	1.36	7.73	0.99	0.17
	313 K	0.61	0.6192	0.95	0.05	24.08	2.51	0.86	1.46	40.90	88.40	2.08	0.99	0.16
HA4	293 K	0.34	0.0941	0.95	0.08	3.60	1.49	0.98	0.27	3.21	−24.86	0.37	0.99	0.68
	303 K	1.09	0.0344	0.92	0.75	4.39	1.26	0.95	0.73	1.64	−76.38	0.09	0.98	14.47
	313 K	0.45	0.2082	0.99	0.44	8.35	1.66	0.99	0.12	9.28	22.84	1.07	0.99	0.01

Table 5 | Thermodynamic parameters of different HA fractions adsorbed on MIEX resin

	ΔH^0	ΔS^0	ΔG^0 (kJ/mol)		
HA	(kJ/mol)	(J /(mol·k))	293 K	303 K	313 K
VHC	0.126	375.4	−109.8	−113.6	−117.4
SHC	0.149	397.2	−116.2	−120.2	−124.2
PHC	0.078	220.5	−64.5	−66.7	−68.9
NHC	0.033	87.9	−25.7	−26.6	−27.5
HA1	0.028	58.8	−17.2	−17.8	−18.4
HA2	0.008	6.4	−1.9	−1.9	−2.0
HA3	0.078	235.2	−68.8	−71.2	−73.5

chemisorption. Table 6 shows that the values of E_a were in the range 8.4–83.7 kJ/mol, indicating that the chemisorption might dominate the adsorption of different HA components (except VHC) on MIEX resin. As for the VHC component, the value of E_a was 94.056 kJ/mol, implying that physical adsorption, such as hydrogen bonding and hydrophobic interaction, might occur in addition to the chemisorption (Phetrak *et al.* 2016).

Table 6 | Activation energy parameters of different HA fractions onto MIEX resin

HA	R^2	E_a (kJ/mol)
VHC	0.91	94.1
SHC	0.47	22.2
PHC	0.99	20.4
NHC	0.99	55.7
HA1	0.88	33.3
HA2	0.96	19.7
HA3	0.86	29.8
HA4	0.99	11.3

4. CONCLUSIONS

The present study explored the adsorption characteristics of HA fractions with different hydrophilic–hydrophobic properties and molecular weights on MIEX resin by a series of batch experiments, and some conclusions were attained as follows. MIEX resin could remove effectively HA components of MW $<$ 10 kDa. In contrast, the hydrophilic components exhibit more preferential affinity onto MIEX resin than hydrophobic components. The influence of solution pH on the removal of MW $<$ 1 kDa fraction could be ignored at the investigated pH 6.0–9.0. However, the removal of other fractions decreased obviously with the pH increase. The time needed to reach equilibrium depended on the organics' characteristics, i.e. molecular weight and/or hydrophobicity. Regardless of HA fractions, the pseudo-second-order model described the adsorption kinetic processes of different HA fractions on MIEX resin well, and the adsorption equilibrium data of HA fractions on MIEX resin could be well fitted with the Sips model. The adsorption of HA fractions on MIEX resin was spontaneous, endothermic and an entropy-driven process. Water samples prepared with commercial humic acid and ultrapure water were used in this study. This might cause a possible risk for guiding the removal of organic matter in actual water. In future research, the removal of HA components in real water and mechanism needs to be studied.

ACKNOWLEDGEMENTS

This work was supported by the National Natural Science Foundation of China (Grant No. 51308001), Anhui Provincial Natural Science Foundation (Grant No. 2108085ME187), and Engineering Research Center of biofilm water purification and utilization technology Ministry of Education (Grant No. BWPU2020KF01) and State Key Laboratory of Pollution Control and Resource Reuse Foundation (Grant No. PCRRF19003).

DATA AVAILABILITY STATEMENT

All relevant data are included in the paper or its Supplementary Information.

REFERENCES

Afshin, S., Rashtbari, Y., Vosough, M., Dargahi, A., Fazlzadeh, M., Behzad, A. & Yousefi, M. 2021 Application of Box-Behnken design for optimizing parameters of hexavalent chromium removal from aqueous solutions using Fe_3O_4 loaded on activated carbon prepared from alga: kinetics and equilibrium study. *Journal Of Water Process Engineering* **42**, 102113.

Allpike, B. P., Heitz, A., Joll, C. A., Kagi, R. I., Abbt-Braun, G., Frimmel, F. H., Brinkmann, T., Her, N. & Amy, G. 2005 Size exclusion chromatography to characterize DOC removal in drinking water treatment. *Environmental Science & Technology* **39** (7), 2334–2342.

Altunterim, R. & Vergili, I. 2020 Clofibric acid removal by ion exchange using a magnetic ion exchange resin: equilibrium, kinetics, reusability and characterisation. *International Journal of Environmental Analytical Chemistry*, doi: 10.1080/03067319.2020.1799998.

Asgharian, F., Khosravi-Nikou, M. R., Anvaripour, B. & Danaee, I. 2017 Electrocoagulation and ultrasonic removal of humic acid from wastewater. *Environmental Progress & Sustainable Energy* **36** (3), 822–829.

Avena, M. J. & Koopal, L. K. 1999 Kinetics of humic acid adsorption at solid-water interfaces. *Environmental Science & Technology* **33** (16), 2739–2744.

Ayub, S., Mohammadi, A. A., Yousefi, M. & Changani, F. 2019 Performance evaluation of agro-based adsorbents for the removal of cadmium from wastewater. *Desalination and Water Treatment* **142**, 293–299.

Banks, J., Fearing, D. A., Guyetand, S., Eroles, C. M., Jefferson, B., Wilson, D. & Parsons, S. A. 2004 Combination of ferric and MIEX for the treatment of a humic rich water. *Water Research* **38** (10), 2551–2558.

Bhaumik, R., Mondal, N. K., Das, B., Roy, P., Pal, K. C., Das, C., Baneerjee, A. & Kumar, D. J. 2015 Eggshell powder as an adsorbent for removal of fluoride from aqueous solution: equilibrium, kinetic and thermodynamic studies. *Journal of Chemistry* **9** (3), 1457–1480.

Bond, T., Goslan, E. H., Parsons, S. A. & Jefferson, B. 2010 Disinfection by-product formation of natural organic matter surrogates and treatment by coagulation, MIEX and nanofiltration. *Water Research* **44** (5), 1645–1653.

Boyer, T. H. & Singer, P. C. 2005 Bench-scale testing of a magnetic ion exchange resin for removal of disinfection by-product precursors. *Water Research* **39** (7), 1265–1276.

Boyer, T. H., Singer, P. C. & Aiken, G. R. 2008 Removal of dissolved organic matter by anion exchange: effect of dissolved organic matter properties. *Environmental Science & Technology* **42** (19), 7431–7437.

Cornelissen, E. R., Beerendonk, E. F., Nederlof, M. N., van der Hoek, J. P. & Wessels, L. P. 2009 Fluidized ion exchange (FIX) to control NOM fouling in ultrafiltration. *Desalination* **236** (1–3), 334–341.

Ding, L., Deng, H., Wu, C. & Han, X. 2012a Affecting factors, equilibrium, kinetics and thermodynamics of bromide removal from aqueous solutions by MIEX resin. *Chemical Engineering Journal* **181**, 360–370.

Ding, L., Wu, C., Deng, H. & Zhang, X. 2012b Adsorptive characteristics of phosphate from aqueous solutions by MIEX resin. *J Colloid Interface* **376** (1), 224–232.

Ding, L., Zhu, Y., Du, B., Ma, J. & Zhang, X. 2017 Removal characteristics of tanic acid adsorbedon MIEX resin. *Polish Journal of Environmental Studies* **26** (3), 1031–1043.

Drikas, M., Dixon, M. & Morran, J. 2011 Long term case study of MIEX pre-treatment in drinking water; understanding NOM removal. *Water Research* **45** (4), 1539–1548.

El-Shahawi, M. S. & Nassif, H. A. 2003 Retention and thermodynamic characteristics of mercury(II) complexes onto polyurethane foams. *Analytica Chimica Acta* **481** (1), 29–39.

Fan, J., Li, H., Shuang, C., Li, W. & Li, A. 2014 Dissolved organic matter removal using magnetic anion exchange resin treatment on biological effluent of textile dyeing wastewater. *Journal of Environmental Ences* **26** (008), 1567–1574.

Geoffrey, B. 2018 Geochemical scaling potential simulations of natural organic matter complexation with metal ions in cooling water at Eskom power generation plants in South Africa. *Water SA* **44** (4), 706–718.

Gibert, O., Pages, N., Bernat, X. & Luis Cortina, J. 2017 Removal of dissolved organic carbon and bromide by a hybrid MIEX-ultrafiltration system: insight into the behaviour of organic fractions. *Chemical Engineering Journal* **312**, 59–76.

Hua, G. & Reckhow, D. A. 2007 Characterization of disinfection byproduct precursors based on hydrophobicity and molecular size. *Environmental Science & Technology* **41** (9), 3309–3315.

Humbert, H., Gallard, H., Suty, H. & Croué, J.-P. 2005 Performance of selected anion exchange resins for the treatment of a high DOC content surface water. *Water Research* **39** (9), 1699–1708.

Largitte, L. & Pasquier, R. 2016 A review of the kinetics adsorption models and their application to the adsorption of lead by an activated carbon. *Chemical Engineering Research & Design: Transactions of the Institution of Chemical Engineers* **109**, 495–504.

Liu, Z., Lompe, K., Mohseni, M., Berube, P. & Barbeau, B. 2020 Biological ion exchange as an alternative to biological activated carbon for drinking water treatment. *Water Research* **168**, 115148.

Llorca, M., Schirinzi, G., Martinez, M., Barcelo, D. & Farre, M. 2018 Adsorption of perfluoroalkyl substances on microplastics under environmental conditions. *Environmental Pollution* **235**, 680–691.

Lu, X., Shao, Y., Gao, N., Chen, J., Wang, Q. & Zhu, Y. 2016 Control of disinfection by-product derived from humic acid using MIEX process: optimization through response surface methodology. *RSC Advances* **6** (85), 82376–82384.

Mergen, M. R. D., Jefferson, B., Parsons, S. A. & Jarvis, P. 2008 Magnetic ion-exchange resin treatment: impact of water type and resin use. *Water Research* **42** (8–9), 1977–1988.

Nguyen, T. V., Zhang, R., Vigneswaran, S., Ngo, H. H., Kandasamy, J. & Mathes, P. 2011 Removal of organic matter from effluents by Magnetic Ion Exchange (MIEX). *Desalination* **276** (1–3), 96–102.

Phetrak, A., Lohwacharin, J., Sakai, H., Murakami, M., Oguma, K., Takizawa, S., Engineering, D. O. U., Engineering, G. S. o., Tokyo, T. U. o. & Science, I. O. I. 2014 Simultaneous removal of dissolved organic matter and bromide from drinking water source by anion exchange resins for controlling disinfection by-products. *Journal of Environmental Sciences* **26** (6), 1294–1300.

Phetrak, A., Lohwacharin, J. & Takizawa, S. 2016 Analysis of trihalomethane precursor removal from sub-tropical reservoir waters by a magnetic ion exchange resin using a combined method of chloride concentration variation and surrogate organic molecules. *Science of the Total Environment* **539**, 165–174.

Rajaei, F., Taheri, E., Hadi, S., Fatehizadeh, A. & Aminabhavi, T. M. 2021 Enhanced removal of humic acid from aqueous solution by combined alternating current electrocoagulation and sulfate radical. *Environmental Pollution* **277**, 116632.

Ren, Z. & Graham, N. 2015 Treatment of humic acid in drinking water by combining potassium manganate (Mn(Vi)), ferrous sulfate, and magnetic ion exchange. *Environmental Engineering Science* **32** (3), 175–178.

Ren, M., Horn, H. & Frimmel, F. H. 2017 Aggregation behavior of TiO_2 nanoparticles in municipal effluent: influence of ionic strengthen and organic compounds. *Water Research* **123**, 678–686.

Schlenger, P., Rodriguez, F. J. & Garcia-Valverde, M. 2016 Monitoring changes in the structure and properties of humic substances following ozonation using UV-vis, FTIR and ^{1}H NMR techniques. *Science of the Total Environment* **541**, 623–631.

Shuang, C., Li, P., Li, A., Zhou, Q., Zhang, M. & Zhou, Y. 2012a Quaternized magnetic microspheres for the efficient removal of reactive dyes. *Water Research* **46** (14), 4417–4426.

Shuang, C., Pan, F., Zhou, Q., Li, A., Li, P. & Yang, W. 2012b Magnetic polyacrylic anion exchange resin: preparation, characterization and adsorption behavior of humic acid. *Industrial & Engineering Chemistry Research* **51** (11), 4380–4387.

Shuang, C., Wang, M., Li, P., Li, A., Zhou, Q., Pan, F. & Zhou, W. 2014 Adsorption of humic acid fractions with different molecular weight by magnetic polyacrylic anion exchange resin. *Journal of Soils & Sediments* **14** (2), 312–319.

Shuang, C., Wang, J., Li, H., Li, A. & Zhou, Q. 2015 Effect of the chemical structure of anion exchange resin on the adsorption of humic acid: behavior and mechanism. *Journal of Colloid & Interface Ence* **437**, 163–169.

Singer, P. C. & Bilyk, K. 2002 Enhanced coagulation using a magnetic ion exchange resin. *Water Research* **36** (16), 4009–4022.

Singh, S. K., Townsend, T. G. & Boyer, T. H. 2012 Evaluation of coagulation ($FeCl_3$) and anion exchange (MIEX) for stabilized landfill leachate treatment and high-pressure membrane pretreatment. *Separation & Purification Technology* **96**, 98–106.

Tan, I. A. W., Ahmad, A. L. & Hameed, B. H. 2009 Adsorption isotherms, kinetics, thermodynamics and desorption studies of 2,4,6-trichlorophenol on oil palm empty fruit bunch-based activated carbon. *Journal of Hazardous Materials* **164** (2–3), 473–482.

Tang, Y., Li, S., Zhang, Y., Yu, S. & Martikka, M. 2014 Sorption of tetrabromobisphenol A from solution onto MIEX resin: batch and column test. *Journal of the Taiwan Institute of Chemical Engineers* **45** (5), 2411–2417.

Torab-Mostaedi, M., Asadollahzadeh, M., Hemmati, A. & Khosravi, A. 2013 Equilibrium, kinetic, and thermodynamic studies for biosorption of cadmium and nickel on grapefruit peel. *Journal of the Taiwan Institute of Chemical Engineers* **44** (2), 295–302.

Tran, H. N., Lima, E. C., Juang, R.-S., Bollinger, J.-C. & Chao, H.-P. 2021 Thermodynamic parameters of liquid–phase adsorption process calculated from different equilibrium constants related to adsorption isotherms: A comparison study. *Journal of Environmental Chemical Engineering* **9** (6), 106674.

Tzabar, N. & Ter Brake, H. J. M. 2016 Adsorption isotherms and sips models of nitrogen, methane, ethane, and propane on commercial activated carbons and polyvinylidene chloride. *Adsorption* **22** (7), 1–14.

Wang, Y., Zhang, X., Zhang, X., Meng, Q., Gao, F. & Zhang, Y. 2017 Characterization of spectral responses of dissolved organic matter (DOM) for atrazine binding during the sorption process onto black soil. *Chemosphere* **180**, 531–539.

Watson, K. & Knight, N. 2014 Enhanced coagulation with powdered activated carbon or MIEX(庐) secondary treatment: a comparison of disinfection by-product formation and precursor removal. *Pediatric Surgery International* **26** (7), 703–706.

Xu, J., Xu, W., Wang, D., Sang, G. & Yang, X. 2016 Evaluation of enhanced coagulation coupled with magnetic ion exchange (MIEX) in natural organic matter and sulfamethoxazole removals: the role of Al-based coagulant characteristic. *Separation and Purification Technology* **167**, 70–78.

Yang, Y., Zheng, Z., Zhang, D. & Zhang, X. 2020 Response surface methodology directed adsorption of chlorate and chlorite onto MIEX resin and study of chemical properties. *Environmental Science: Water Research & Technology* **6** (9), 2454–2464.

Zhang, R., Vigneswaran, S., Ngo, H. H. & Nguyen, H. 2006 Magnetic ion exchange (MIEX®) resin as a pre-treatment to a submerged membrane system in the treatment of biologically treated wastewater. *Desalination* **192** (1–3), 296–302.

Zhang, Y., Chu, W., Yao, D. & Yin, D. 2017 Control of aliphatic halogenated DBP precursors with multiple drinking water treatment processes: formation potential and integrated toxicity. *Journal of Environmental Sciences* **58**, 322–330.

First received 4 November 2021; accepted in revised form 17 February 2022. Available online 2 March 2022